Synthesis of "Phosphine Tethered" η^2-Allene and μ-η^1:η^2-Alkenyl Complexes: Facile P−C_α Bond Formation and C−H Activation Reactions of Bis(diphenylphosphino)methane with $[Fe_2(CO)_6(\mu\text{-}ER)\{\mu\text{-}\eta^1\text{:}\eta^2{}_{\alpha,\beta}\text{-}(H)C_\alpha{=}C_\beta{=}C_\gamma H_2\}]$ (E = PPh, R = Ph; E = S, R = ^{t}Bu)

Simon Doherty,*,† Mark R. J. Elsegood, William Clegg, Dirk Mampe, and Nicholas H. Rees

Department of Chemistry, Bedson Building, The University of Newcastle upon Tyne, Newcastle upon Tyne NE1 7RU, United Kingdom

Received June 21, 1996⊗

The phosphido-bridged diiron allenyl complex $[Fe_2(CO)_6(\mu\text{-}PPh_2)\{\mu\text{-}\eta^1\text{:}\eta^2{}_{\alpha,\beta}\text{-}(H)C_\alpha{=}C_\beta{=}C_\gamma H_2\}]$ (**1**) reacts with dppm to afford, in the first instance, $[Fe_2(CO)_6(\mu\text{-}PPh_2)\{\eta^1(P)\text{:}\eta^2(C)\text{-}Ph_2PCH_2PPh_2(H)C{=}C{=}CH_2\}]$ (**3**), which contains a novel $\eta^1(P)$:$\eta^2(C)$-dppm-functionalized allene. A single-crystal X-ray study reveals **3** to be derived from **1** by nucleophilic attack of dppm at C_α with metal−metal bond cleavage and internuclear migration of CO. Upon standing in toluene $[Fe_2(CO)_6(\mu\text{-}PPh_2)\{\eta^1(P)\text{:}\eta^2(C)\text{-}Ph_2PCH_2PPh_2(H)C{=}C{=}CH_2\}]$ (**3**) slowly decarbonylates to afford the unusual σ-π-alkenyl complex $[Fe_2(CO)_5(\mu\text{-}PPh_2)\{\mu\text{-}\eta^1(P)\text{:}\eta^1(C)\text{:}\eta^2(C)\text{-}Ph_2PCHPPh_2(H)C{=}CCH_3\}]$ (**4**), containing a metal- and carbon-coordinated bis(diphenylphosphino)methanide ligand. Overall, the transformation of **3** into **4** requires activation of a dppm methylene C−H bond, hydrogen migration to C_γ together with metal−metal bond formation, and loss of CO. Surprisingly, $[Fe_2(CO)_6(\mu\text{-}S^tBu)\{\mu\text{-}\eta^1\text{:}\eta^2{}_{\alpha,\beta}\text{-}(H)C_\alpha{=}C_\beta{=}C_\gamma H_2\}]$ and dppm react to afford high yields of the isomeric alkenyl complexes $[Fe_2(CO)_5(\mu\text{-}S^tBu)\{\mu\text{-}\eta^1(P)\text{:}\eta^1(C)\text{:}\eta^2(C)\text{-}Ph_2PCHPPh_2(H)C{=}CCH_3\}]$ (**5a**; 90%) and $[Fe_2(CO)_5(\mu\text{-}S^tBu)\{\mu\text{-}\eta^1(P)\text{:}\eta^1(C)\text{:}\eta^2(C)\text{-}Ph_2PCHPPh_2\text{-}CH_2C{=}CH_2\}]$ (**5b**; 10%), the former of which is a structural analogue of $[Fe_2(CO)_5(\mu\text{-}PPh_2)\{\mu\text{-}\eta^1(P)\text{:}\eta^1(C)\text{:}\eta^2(C)\text{-}Ph_2PCHPPh_2(H)C{=}CCH_3\}]$ (**4**). We tentatively suggest that **5a** and **5b** form *via* C−H activation and hydrogen migration in an η^2-allene intermediate similar to **3** with the final isomeric distribution depending upon the regiochemistry of the hydrogen migration step, namely to C_α or C_γ. Full structural details of **3**, **4**, **5a**, and **5b** are reported.

Introduction

By far the most common role for bis(diphenylphosphino)methane (dppm) is that of a bridging ligand, and as such it has found widespread use as a versatile supporting ligand in an impressive array of complexes.[1] However, a growing number of reports suggest that dppm has a rich and varied chemistry far beyond that of an innocent spectator ligand. Indeed, recent years have witnessed some quite remarkable observations, including facile P−C bond cleavage reactions,[2] metalation of the aromatic C−H bonds,[3] competitive nucleophilic attack between carbon and metal atoms in binuclear hydrocarbyl-bridged complexes,[4,5] and recently, intramolecular nucleophilic attack of one end of a dppm at a μ-η^1:η^1-coordinated alkyne.[6] Although there have been relatively few reports of nucleophilic attack between bidentate phosphines and unsaturated hydrocarbyl ligands,[4−6] P−C bond formation involving monofunctional phosphines is well-documented.[7]

We have recently initiated a systematic investigation into the reactivity of the diiron allenyl complexes $[Fe_2(CO)_6(\mu\text{-}ER)\{\mu\text{-}\eta^1\text{:}\eta^2{}_{\alpha,\beta}\text{-}(H)C_\alpha{=}C_\beta{=}C_\gamma H_2\}]$ (E = PPh, R = Ph, **1**; E = S, R = ^{t}Bu, **2**), and our efforts in this area have unveiled a wealth of unexpected reactivity toward monofunctional nucleophiles, including the generation of amido-functionalized alkenyl complexes *via* a novel amine−carbonyl−allenyl coupling sequence[8] and an unprecedented nucleophilic attack of primary and secondary phosphines at C_α to afford, after 1,4-hydrogen migration, new phosphino-substituted μ-η^1:η^2-alkenyl ligands.[9] In addition to these studies we are currently examining the reactivity of **1** and **2** with dppm to compare with $[Ru_2(CO)_6(\mu\text{-}PPh_2)\{\mu\text{-}\eta^1\text{:}\eta^2\text{-}(Ph)C_\alpha{=}C_\beta{=}C_\gamma H_2\}]$, which was reported to react *via* allenyl−carbonyl−phosphido coupling to afford a novel ketoallenyl

† E-mail: simon.doherty@newcastle.ac.uk.

⊗ Abstract published in *Advance ACS Abstracts,* November 15, 1996.

(1) (a) Puddephatt, R. J. *Chem. Soc. Rev.* **1983**, *12*, 99. (b) Chaudret, B.; Delavaux, B.; Poiblanc, R. *Coord. Chem. Rev.* **1988**, *86*, 191.

(2) (a) Hogarth, G.; Knox, S. A. R.; Turner, M. L. *J. Chem. Soc., Chem. Commun.* **1990**, 145. (b) Hogarth, G.; Knox, S. A. R.; MacPherson, K. A.; Melchior, F.; Morton, D. A. V.; Orpen, A. G. *Inorg. Chim. Acta* **1992**, *198−200*, 257. (c) Hogarth, G.; Knox, S. A. R.; Turner, M. L. *J. Chem. Soc., Chem. Commun.* **1990**, 145.

(3) Doherty, N. M.; Hogarth, G.; Knox, S. A. R.; Macpherson, K. A.; Melchior, F.; Orpen, A. G. *J. Chem. Soc., Chem. Commun.* **1986**, 540.

(4) Hogarth, G.; Knox, S. A. R.; Lloyd, B. R. L.; Macpherson, K. A.; Melchior, F.; Morton, D. A. V.; Orpen, A. G. *J. Chem. Soc., Chem. Commun.* **1988**, 360.

(5) Cherkas, A. A.; Doherty, S.; Cleroux, M.; Hogarth, G.; Randall, L. H.; Breckenridge, S. M.; Taylor, N. J.; Carty, A. J. *Organometallics* **1992**, *11*, 1701.

(6) Antwi-Nsiah, F. H.; Oke, O.; Cowie, M. *Organometallics* **1996**, *15*, 506.

S0276-7333(96)00502-X CCC: $12.00

phosphine.[10] Herein we describe a new reaction pathway for bis(diphenylphosphino)methane with σ-η-allenyl complexes, which involves P—C_α bond formation together with activation of a dppm methylene C—H bond, and hydrogen migration to the coordinated allenyl ligand. Both **1** and **2** react with dppm to ultimately afford the bis(diphenylphosphino)methanide-tethered μ-η^1:η^2-alkenyl complexes **[**$Fe_2(CO)_5(\mu\text{-ER})\{\mu\text{-}\eta^1(P)\text{:}\eta^1(C)\text{:}\eta^2(C)\text{-}Ph_2PCHPPh_2(H)C{=}CCH_3\}$] (**4**, E = PPh, R = Ph; **5a**, E = S, R = ^{t}Bu) and $[Fe_2(CO)_5(\mu\text{-ER})\{\mu\text{-}\eta^1(P)\text{:}\eta^1(C)\text{:}\eta^2(C)\text{-}Ph_2PCHPPh_2CH_2C{=}CH_2\}]$ (**5b**, E = S, R = ^{t}Bu), although in the case of $[Fe_2(CO)_6(\mu\text{-}PPh_2)\{\mu\text{-}\eta^1\text{:}\eta^2{}_{\alpha,\beta}\text{-}(H)\text{-}C_\alpha{=}C_\beta{=}C_\gamma H_2\}]$ (**1**) nucleophilic attack at C_α of the allenyl ligand initially affords the intermediate $[Fe_2(CO)_6(\mu\text{-}PPh_2)\{\eta^1(P)\text{:}\eta^2(C)\text{-}Ph_2PCH_2PPh_2(H)C{=}C{=}CH_2\}]$ (**3**), which contains an $\eta^1(P)$:$\eta^2(C)$-coordinated dppm-functionalized allene. The bis(diphenylphosphino)methanide anion, formally derived from dppm by deprotonation, is increasing in popularity as a coordinatively and electronically versatile ligand for transition metals in a variety of oxidation states, and such complexes are generally accessed *via* metathesis routes[11] or deprotonation of a coordinated dppm.[12] The generation of **4**, **5a**, and **5b** represents, to the best of our knowledge, the first examples of a facile C—H bond activation—hydrogen migration pathway during the reaction of dppm with a σ-η-hydrocarbyl complex.

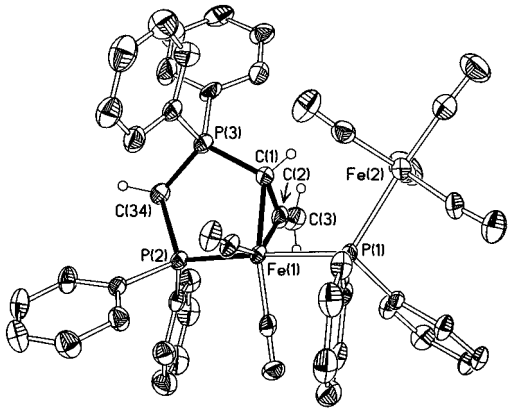

Figure 1. Molecular structure of $[Fe_2(CO)_6(\mu\text{-}PPh_2)\{\eta^1(P)\text{:}\eta^2(C)\text{-}Ph_2PCH_2PPh_2(H)C{=}C{=}CH_2\}]$ (**3**), illustrating the η^1-(P):$\eta^2(C)$ "phosphine tethered" allene ligand. Phenyl hydrogen atoms have been omitted. Ellipsoids are at the 50% probability level.

Results and Discussion

Reaction of $[Fe_2(CO)_6(\mu\text{-}PPh_2)\{\mu\text{-}\eta^1\text{:}\eta^2{}_{\alpha,\beta}\text{-}(H)\text{-}C_\alpha{=}C_\beta{=}C_\gamma H_2\}]$ with dppm: Synthesis and Characterization of $[Fe_2(CO)_5(\mu\text{-}PPh_2)\{\mu\text{-}\eta^1(P)\text{:}\eta^2(C)\text{:}\eta^2(C)\text{-}Ph_2PCHPPh_2(H)C{=}CCH_3\}]$ (3) and $[Fe_2(CO)_5(\mu\text{-}PPh_2)\{\mu\text{-}\eta^1(P)\text{:}\eta^1(C)\text{:}\eta^2(C)\text{-}Ph_2PCHPPh_2\text{-}CH_2C{=}CH_2\}]$ (4). The diiron allenyl complex $[Fe_2(CO)_6(\mu\text{-}PPh_2)\{\mu\text{-}\eta^1\text{:}\eta^2{}_{\alpha,\beta}\text{-}(H)C_\alpha{=}C_\beta{=}C_\gamma H_2\}]$ (**1**) reacts with dppm, in toluene/diethyl ether, to afford $[Fe_2(CO)_6(\mu\text{-}PPh_2)\{\eta^1(P)\text{:}\eta^2(C)\text{-}Ph_2PCH_2PPh_2(H)C{=}C{=}CH_2\}]$ (**3**), which crystallizes directly from the reaction mixture in yields of up to 60%. As expected, the $^{31}P\{^1H\}$ NMR spectrum of **3** contains three distinct mutually coupled resonances (δ 75.6, 73.7, 37.8 ppm (ABX)). Of these, the two at low field are associated with the bridging phosphido ligand and the metal-coordinated diphosphine, the former of which appears in the region most commonly associated with μ-PPh_2 bridging nonbonded metal atoms.[13] The remaining high-field signal is characteristic of a carbon-coordinated diphosphine.[5] All three ^{13}C signals associated with the C_3-bridging ligand have been identified, two of which have chemical shifts close to those of C_β and C_γ in **1**[9] (**3**, δ 176.5, 119.0; **1**, δ 180.0, 79.0 ppm), while the remaining signal, that associated with C_α, is shifted to high field (**3**, δ 18.4 ppm, $^1J_{PC}$ = 76.0 Hz; **1**, δ 118.3 ppm). These spectroscopic features suggest that the reaction of **1** with dppm occurs with P—C bond formation, retention of the uncoordinated C—C double bond, and metal—metal bond cleavage. However, beyond this, the exact nature of **3** remained uncertain and a single-crystal X-ray study was undertaken to provide full structural details.

The results of the structural study are presented in Figure 1 with a selection of bond distances and angles listed in Table 1. The most remarkable feature of this structure is the transformation of a μ-η^1:η^2-allenyl ligand into a $\eta^1(P)$:$\eta^2(C)$-coordinated dppm-functionalized allene (C(1)—P(3) = 1.753(6) Å, Fe(1)—C(1) = 2.030(6) Å, Fe(1)—C(2) = 1.942(6) Å). Overall, formation of **3** requires P—C_α bond formation, cleavage of the Fe—Fe bond, redistribution of the carbonyl ligands, and η^2-

(7) For alkyne complexes: (a) Takats, J.; Washington, L.; Santarsiero, B. D. *Organometallics* **1994**, *13*, 1078. For cyclopentadienone complexes: (b) Slugovc, C.; Mauthner, K.; Mereiter, K.; Schmid, R.; Kirchner, K. *Organometallics* **1996**, *15*, 2954. For acetylide complexes: (c) Cherkas, A. A.; Breckenridge, S. M.; Carty, A. J. *Polyhedron* **1991**, *11*, 1075. (d) Cherkas, A. A.; Randall, L. H.; Taylor, N. J.; Mott, G. N.; Yule, J. E.; Guinamant, J. L.; Carty, A. J. *Organometallics* **1990**, *9*, 1677. (e) Nucciarone, D.; Taylor, N. J.; Carty, A. J. *Organometallics* **1986**, *5*, 1179. (f) Cherkas, A. A.; Mott, G. N.; Granby, R.; MacLaughlin, S. A.; Yule, J. G.; Taylor, N. J.; Carty, A. J. *Organometallics* **1988**, *7*, 1115. (g) Seyferth, S.; Hoke, J. B.; Wheeler, D. R. *J. Organomet. Chem.* **1988**, *341*, 421. (h) Boyar, E.; Deeming, A. J.; Kabir, S. E. *J. Chem. Soc., Chem. Commun.* **1986**, 577. (i) Deeming, A. J.; Hasso, S. *J. Organomet. Chem.* **1976**, *112*, C39. (j) Deeming, A. J.; Manning, P. *J. Organomet. Chem.* **1984**, *265*, 87. For vinylidenes: (k) Bruce, M. I. *Chem. Rev.* **1991**, *91*, 197. For carbenes and carbynes: (l) Kreissl, F. R.; Hel, W. *Chem. Ber.* **1977**, *110*, 799. (m) Fischer, E. O.; Reitmeier, R.; Ackermann, K. *Angew. Chem., Int. Ed. Engl.* **1983**, *22*, 411. (n) Kreissl, F. R.; Friedrich, P. *Angew. Chem., Int. Ed. Engl.* **1977**, *16*, 543. (o) Kreissl, F. R.; Stuckler, P.; Meineke, E. W. *Chem. Ber.* **1977**, *110*, 3040. (p) Fischer, E. O.; Ruhs, A.; Kreissl, F. R. *Chem. Ber.* **1977**, *110*, 805. (q) Busetto, L.; Carlucci, L.; Zanotti, V.; Albano, V. G.; Monari, M. *Chem. Ber.* **1992**, *125*, 1125. (r) Bassi, M.; Carlucci, L.; Zanotti, V. *Inorg. Chim. Acta* **1993**, *204*, 171. For allenyl and propargyl complexes: (s) Casey, C. P.; Yi, C.-S. *J. Am. Chem. Soc.* **1992**, *114*, 6597. (t) Henrick, K.; McPartlin, M.; Deeming, A. J.; Hasso, S.; Manning, P. *J. Chem. Soc., Dalton Trans.* **1982**, 899. (u) Breckenridge, S. M.; Taylor, N. J.; Carty, A. J. *Organometallics* **1991**, *10*, 837.

(8) Doherty, S.; Elsegood, M. R. J.; Clegg, W.; Waugh, M. *Organometallics* **1996**, *15*, 2688.

(9) Doherty, S.; Elsegood, M. R. J.; Clegg, W.; Scanlan, T.; Rees, N. H. *J. Chem. Soc. Chem. Commun.* **1996**, 1545.

(10) Carleton, N.; Corrigan, J. F.; Doherty, S.; Pixneur, R.; Sun, Y.; Taylor, N. J.; Carty, A. J. *Organometallics* **1994**, *13*, 4179.

(11) (a) Karsch, H. H.; Grauvogl, G.; Kawecki, M.; Bissinger, P.; Kumberger, O.; Schier, A.; Muller, G. *Organometallics* **1994**, *13*, 610. (b) Karsch, H. H.; Grauvogl, G.; Deubelly, B.; Muller, G. *Organometallics* **1992**, *11*, 4238. (c) Karsch, H. H.; Deubelly, B.; Grauvogl, G.; Lachmann, J.; Muller, G. *Organometallics* **1992**, *11*, 4245. (d) Karsch, H. H.; Appelt, A.; Muller, G. *Angew. Chem., Int. Ed. Engl.* **1986**, *25*, 823.

(12) (a) Laguna, A.; Laguna, M. *J. Organomet. Chem.* **1990**, *394*, 743. (b) Li, J.-J.; Sharp, P. R. *Inorg. Chem.* **1996**, *35*, 604. (c) Li, J. J.; Sharp, P. R. *Inorg. Chem.* **1994**, *33*, 183. (d) Ruiz, J.; Riera, V.; Vivanco, M.; Garcia-Granda, S.; Salvado, M. A. *Organometallics* **1996**, *15*, 1079. (e) Ruiz, J.; Arauz, R.; Riera, V.; Vivanco, M.; Garcia-Granda, S.; Menendez-Velazquez, A. *Organometallics* **1994**, *13*, 4162. (f) Ruiz, J.; Riera, V.; Vivanco, M.; Garcia-Granda, S.; Garcia-Fernandez, A. *Organometallics* **1992**, *11*, 4077. (g) Dawkins, G. M.; Green, M.; Jeffrey, J. C.; Sambale, C.; Stone, F. G. A. *J. Chem. Soc., Dalton Trans.* **1983**, 499.

(13) MacLaughlin, S. A.; Nucciarone, D.; Carty, A. J. In *Phosphorus-31 NMR Spectroscopy in Stereochemical Analysis*; Verkade, J. G., Quinn, L. D., Eds.; Organic Compounds and Metal Complexes; VCH: New York, 1987; Chapter 16.

Table 1. Selected Bond Distances (Å) and Angles (deg) for Compound 3

Fe(1)−C(1)	2.030(6)	Fe(1)−C(2)	1.942(6)
Fe(1)−P(1)	2.356(2)	Fe(1)−P(2)	2.218(2)
P(2)−C(34)	1.853(6)	C(1)−P(3)	1.753(6)
P(3)−C(34)	1.801(6)	C(1)−C(2)	1.445(9)
C(2)−C(3)	1.305(9)		
Fe(2)−P(1)−Fe(1)	121.70(7)	C(3)−C(2)−C(1)	137.4(6)
P(2)−Fe(1)−P(1)	175.37(7)	C(34)−P(2)−Fe(1)	108.7(2)
P(3)−C(34)−P(2)	108.8(3)	C(1)−P(3)−C(34)	106.2(3)
P(3)−C(1)−Fe(1)	114.7(3)	C(1)−Fe(1)−P(2)	90.0(2)
C(2)−C(1)−P(3)	117.5(5)		

coordination of the allene ligand. Atoms Fe(1), P(2), C(34), P(3), and C(1) form a five-membered saturated ring system and, since P(3) is attached to four carbon atoms, it is zwitterionic with the negative charge delocalized onto the iron atoms. The C(1)−C(2) bond length (1.445(9) Å) shows the expected increase upon coordination and is comparable to values in other allene complexes.[14] The dihedral angle of 89.8° between the planes defined by P(3), C(1), H(1) and H(3a), C(3), H(3b) reflects the allenic character of this modified hydrocarbyl fragment (all these hydrogens were freely refined), although there is a significant deviation of C(1)C(2)C(3) from linearity (137.4(6)°). This, we believe, is the first example of P−C bond formation between a μ-η^1:η^2-allenyl ligand and a diphosphine; in fact, P−C bond formation between dppm and σ-η-hydrocarbyl ligands is not a common reaction pathway. Two such complexes, $[Fe_2(CO)_6\{\mu\text{-}C(CH_2)P(Ph_2)CH_2PPh_2\}]$[4] and $[Fe_2(CO)_5(\mu\text{-}PPh_2)\{\mu\text{-}C{=}C(Ph)Ph_2PCH_2PPh_2\}]$,[5] have been structurally characterized, both of which contain a carbon- and metal-bonded diphosphine, although thermolysis of the latter in toluene readily leads to P−C bond cleavage, elimination of CO, and formation of the disubstituted complex $[Fe_2(CO)_4(\mu\text{-}PPh_2)(\mu\text{-dppm})(\mu\text{-}\eta^1{:}\eta^2\text{-}C{=}CPh)]$. We have found complex **2** to be stable with respect to P−C bond cleavage, and our efforts to transform it into $[Fe_2(CO)_4(\mu\text{-}PPh_2)(\mu\text{-dppm})\{\mu\text{-}\eta^1{:}\eta^2\text{-}(H)C_\alpha{=}C_\beta{=}C_\gamma H_2\}]$ by heating a toluene solution at 80 °C overnight have proven unsuccessful.

Surprisingly, upon standing, toluene solutions of **3** smoothly decarbonylate to form **[**$Fe_2(CO)_5(\mu\text{-}PPh_2)\{\mu\text{-}\eta^1(P){:}\eta^1(C){:}\eta^2(C)\text{-}Ph_2PCHPPh_2(H)C{=}CCH_3\}$] (**4**), readily identified by the appearance of a new set of resonances in the $^{31}P\{^1H\}$ NMR spectrum of the reaction mixture. One of these, a low-field doublet of doublets (δ 185.5, $^2J_{PP}$ = 63.0, 39.0 Hz), appears in the region commonly encountered for μ-PPh_2 ligands bridging metal−metal bonds.[13] The remaining two sets of resonances, both doublets of doublets, are relatively unshifted, which suggests little or no change in the mode of coordination of dppm, although the phosphorus−phosphorus coupling constant of 122.0 Hz is substantially larger than in **3**. In addition, the $^{13}C\{^1H\}$ NMR spectrum of **4** provides further support for retention of the metal−carbon coordinated dppm in the form of a low-field resonance (δ 57.7 ppm) with a relatively large phosphorus−carbon coupling constant ($^1J_{PC}$ = 75.0 Hz). The $^{13}C\{^1H\}$ NMR spectrum of **4** also contains an unusually high field shifted doublet of doublets at δ 7.8 with exceptionally large phosphorus−carbon coupling constants ($^1J_{PC}$ = 133.4, 63.7 Hz). Finally, the apparent absence of both

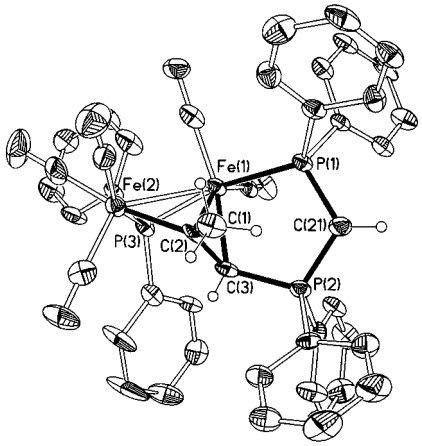

Figure 2. Molecular structure of $[Fe_2(CO)_5(\mu\text{-}PPh_2)\{\mu\text{-}\eta^1(P){:}\eta^1(C){:}\eta^2(C)\text{-}Ph_2PC(H)PPh_2(H)C{=}CCH_3\}]$ (**4**), highlighting the bis(diphenylphosphino)methanide-functionalized σ-π-alkenyl ligand. Phenyl hydrogens have been omitted.

Table 2. Selected Bond Distances (Å) and Angles (deg) for Compound 4

Fe(1)−Fe(2)	2.6050(12)	Fe(1)−C(2)	2.075(6)
Fe(1)−C(3)	2.099(6)	Fe(2)−C(2)	2.002(6)
Fe(1)−P(1)	2.2683(17)	Fe(1)−P(3)	2.2263(17)
Fe(2)−P(3)	2.2169(19)	P(1)−C(21)	1.723(6)
P(2)−C(21)	1.696(6)	C(3)−P(2)	1.789(6)
C(1)−C(2)	1.497(8)	C(2)−C(3)	1.431(8)
Fe(2)−P(3)−Fe(1)	71.79(6)	P(3)−Fe(1)−P(1)	167.62(7)
C(21)−P(1)−Fe(1)	108.2(2)	P(2)−C(21)−P(1)	116.4(3)
C(21)−P(2)−C(3)	107.9(3)	P(2)−C(3)−Fe(1)	114.0(3)
C(3)−Fe(1)−P(1)	87.39(17)	C(3)−C(2)−C(1)	119.8(5)
C(3)−Fe(1)−P(3)	83.31(17)		

dppm and allenyl methylene groups in **4**, supported by DEPT and $^{13}C\{^1H\}-^1H$ correlated NMR experiments, prompted us to undertake a single-crystal X-ray study in order to reveal the precise nature of this transformation.

A perspective view of the molecular structure together with the atomic numbering scheme is illustrated in Figure 2 with a selection of bond distances and angles listed in Table 2. First and foremost we note the presence of a metal- and carbon-bonded dppm in **4** (Fe(1)−P(1) = 2.2683(17) Å, P(2)−C(3) = 1.789(6) Å) and a μ-PPh_2 bridging a metal−metal bond (Fe(1)−Fe(2) = 2.6050(12) Å), structural characteristics that readily account for the $^{31}P\{^1H\}$ NMR data. The most remarkable feature of this structure is the transformation of a $\eta^1(P){:}\eta^2(C)$-dppm-functionalized allene into a bis(diphenylphosphino)methanide-tethered μ-η^1:η^2-alkenyl group σ-bonded to Fe(2) (Fe(2)−C(2) = 2.002(6) Å) and π-bonded to Fe(1) (Fe(1)−C(2) = 2.075(6) Å, Fe(1)−C(3) = 2.099(6) Å). The alkenyl ligand in **4** adopts an *endo* conformation with respect to the phosphido bridge[15] and is tethered to Fe(1) by coordination of the bis(diphenylphosphino)methanide. Atoms P(2), C(21), P(1), Fe(1), and C(3) form a partially unsaturated five-membered ring comprising the bis(diphenylphosphino)methanide fragment, C_β of the σ-π-alkenyl ligand (formally C_α of the allenyl ligand), and Fe(1) (Scheme 1). The bis(diphenylphosphino)methanide shows the expected contraction in P−C bond length (P(1)−C(21) = 1.723(6) Å, P(2)−C(21) = 1.696(6) Å) due to partial

(14) Barry, J. T.; Chacon, S. T.; Chisholm, M. H.; Huffman, J. C.; Streib, W. *J. Am. Chem. Soc.* **1995**, *117*, 1974.

(15) MacLaughlin, S. A.; Doherty, S.; Taylor, N. J. Carty, A. J. *Organometallics* **1992**, *11*, 4315.

Scheme 1

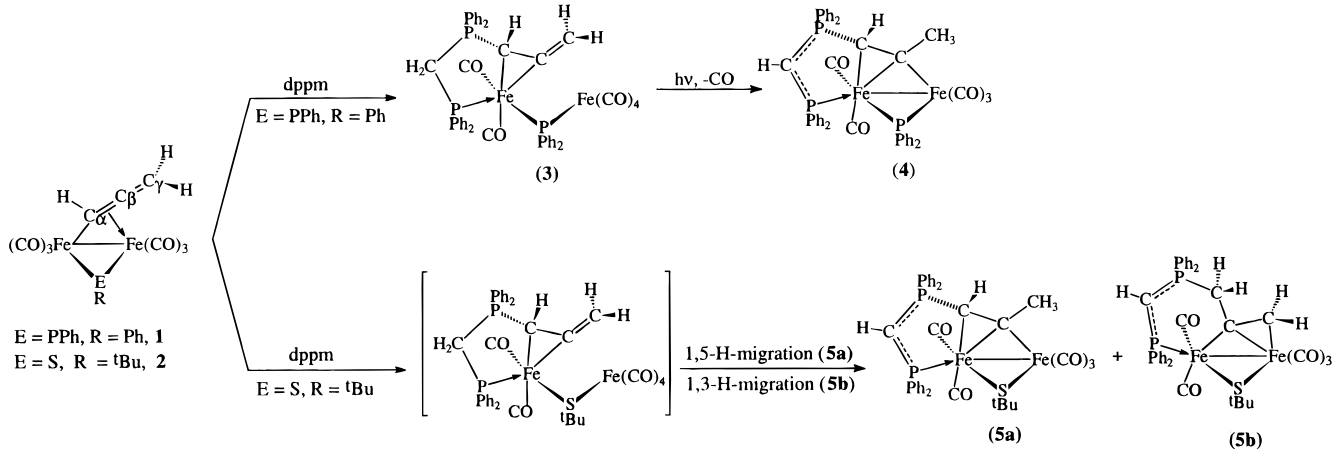

multiple-bond character within the PCP framework.[11,12] Overall, the transformation of **3** into **4** involves activation of a dppm methylene C−H bond together with a 1,5-hydrogen migration to C_γ (C(1)), re-formation of the metal−metal bond, and elimination of carbon monoxide.

Reaction of $[Fe_2(CO)_6(\mu\text{-}S^tBu)\{\mu\text{-}\eta^1\text{:}\eta^2_{\alpha,\beta}\text{-}(H)C_\alpha{=}C_\beta{=}C_\gamma H_2\}]$ with dppm: Synthesis and X-ray Structures of $[Fe_2(CO)_5(\mu\text{-}S^tBu)\{\mu\text{-}\eta^1(P)\text{:}\eta^1(C)\text{:}\eta^2(C)\text{-}Ph_2PCHPPh_2(H)C{=}CCH_3\}]$ (5a) and $[Fe_2(CO)_5(\mu\text{-}S^tBu)\{\mu\text{-}\eta^1(P)\text{:}\eta^1(C)\text{:}\eta^2(C)\text{-}Ph_2PCHPPh_2\text{-}CH_2C{=}CH_2\}]$ (5b). Our efforts to extend this chemistry to the sulfido-bridged complex $[Fe_2(CO)_6(\mu\text{-}S^tBu)\{\mu\text{-}\eta^1\text{:}\eta^2\text{-}(H)C_\alpha{=}C_\beta{=}C_\gamma H_2\}]$ (**2**) resulted in the unexpected isolation of the isomeric bis(diphenylphosphino)-methanide-functionalized $\mu\text{-}\eta^1\text{:}\eta^2$-alkenyl complexes $[Fe_2(CO)_5(\mu\text{-}S^tBu)\{\mu\text{-}\eta^1(P)\text{:}\eta^1(C)\text{:}\eta^2(C)\text{-}Ph_2PCHPPh_2\text{-}(H)C{=}CCH_3\}]$ (**5a)** and $[Fe_2(CO)_5(\mu\text{-}S^tBu)\{\mu\text{-}\eta^1(P)\text{:}\eta^1(C)\text{:}\eta^2(C)\text{-}Ph_2PCHPPh_2CH_2C{=}CH_2\}]$ (**5b**). Treatment of a diethyl ether solution of **2** with dppm at 298 K resulted in the instantaneous formation of a deep red solution. Removal of the solvent, extraction into hexane, and crystallization at 0 °C yielded X-ray-quality crystals of deep red $[Fe_2(CO)_5(\mu\text{-}S^tBu)\{\mu\text{-}\eta^1(P)\text{:}\eta^1(C)\text{:}\eta^2(C)\text{-}Ph_2\text{-}PCHPPh_2(H)C{=}CCH_3\}]$ (**5a**; 90%) and orange $[Fe_2\text{-}(CO)_5(\mu\text{-}S^tBu)\{\mu\text{-}\eta^1(P)\text{:}\eta^1(C)\text{:}\eta^2(C)\text{-}Ph_2PCHPPh_2\text{-}CH_2C{=}CH_2\}]$ (**5b**; 10%). The $^{31}P\{^1H\}$ characteristics of **5a** and **5b** (**5a**, 61.8, 25.9 ppm, $^2J_{PP}$ = 112.0 Hz; **5b**, 60.6, 30.4 ppm, $^2J_{PP}$ = 72.0 Hz) leave little doubt that both complexes contain a metal- and carbon-coordinated bis(diphenylphosphino)methanide. Moreover, the $^{13}C\text{-}\{^1H\}$ NMR spectrum of **5a** contained a high-field-shifted doublet of doublets at δ 8.6 with coupling constants similar in magnitude to those previously reported for this ligand type.[11,12] Unfortunately, the low isolated yields of **5b** prevented us from obtaining its $^{13}C\{^1H\}$ NMR spectrum, and on the basis of ^1H NMR data alone we were unable to arrive at a reasonable formulation. However, the precise identity of both **5a** and **5b** were finally underpinned with single-crystal X-ray studies.

A single-crystal X-ray study of **5a** was undertaken to compare with that of **4**. Compound **5a** crystallizes with two independent but essentially identical molecules in the asymmetric unit of the monoclinic cell, and the following discussion is based on data for molecule A. A perspective view of the molecular structure of **5a** is presented in Figure 3, while Table 3 lists a selection of bond distances and angles for both molecules A and B. The molecular structure identifies **5a** as $[Fe_2(CO)_5(\mu\text{-}S^tBu)\{\mu\text{-}\eta^1(P)\text{:}\eta^1(C)\text{:}\eta^2(C)\text{-}Ph_2PCHPPh_2(H)C{=}CCH_3\}]$, for which the principal feature of interest is the bis-(diphenylphosphino)methanide-functionalized $\mu\text{-}\eta^1\text{:}\eta^2$-

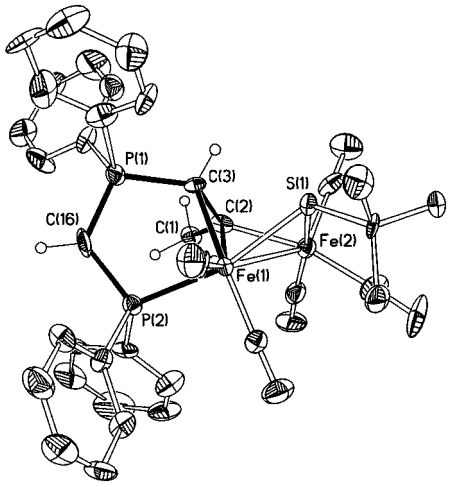

Figure 3. Molecular structure of $[Fe_2(CO)_5(\mu\text{-}S^tBu)\{\mu\text{-}\eta^1(P)\text{:}\eta^1(C)\text{:}\eta^2(C)\text{-}Ph_2PC(H)PPh_2(H)C{=}CCH_3\}]$ (**5a**, molecule A), illustrating the five-membered-ring system formed by iron and carbon coordination of dppm. Phenyl and *tert*-butyl hydrogens have been omitted.

Table 3. Selected Bond Distances (Å) and Angles (deg) for Compound 5a

molecule A		molecule B	
Fe(1)−Fe(2)	2.548(2)	Fe(3)−Fe(4)	2.572(2)
Fe(1)−C(2)	2.072(11)	Fe(3)−C(39)	2.088(12)
Fe(1)−C(3)	2.106(11)	Fe(3)−C(40)	2.101(12)
Fe(2)−C(2)	2.017(12)	Fe(4)−C(39)	1.969(12)
Fe(1)−P(2)	2.249(3)	Fe(3)−P(4)	2.240(3)
Fe(1)−S(1)	2.273(3)	Fe(3)−S(2)	2.283(3)
Fe(2)−S(1)	2.257(3)	Fe(4)−S(2)	2.262(4)
P(2)−C(16)	1.730(14)	P(4)−C(53)	1.756(12)
P(1)−C(16)	1.661(13)	P(3)−C(53)	1.638(13)
C(3)−P(1)	1.786(12)	C(40)−P(3)	1.805(12)
C(1)−C(2)	1.491(16)	C(38)−C(39)	1.507(17)
C(2)−C(3)	1.427(16)	C(39)−C(40)	1.446(18)
Fe(2)−S(1)−Fe(1)	68.46(10)	Fe(4)−S(2)−Fe(3)	68.92(10)
P(2)−Fe(1)−S(1)	165.98(14)	P(4)−Fe(3)−S(2)	165.77(14)
P(1)−C(3)−Fe(1)	112.2(5)	P(3)−C(40)−Fe(3)	111.5(6)
C(16)−P(1)−C(3)	107.7(6)	C(53)−P(3)−C(40)	108.1(6)
P(1)−C(16)−P(2)	117.8(7)	P(3)−C(53)−P(4)	117.7(7)
C(16)−P(2)−Fe(1)	105.5(4)	C(53)−P(4)−Fe(3)	105.5(4)
C(3)−Fe(1)−P(2)	87.5(3)	C(40)−Fe(3)−P(4)	88.2(3)
C(1)−C(2)−C(3)	119.0(10)	C(38)−C(39)−C(40)	117.2(11)

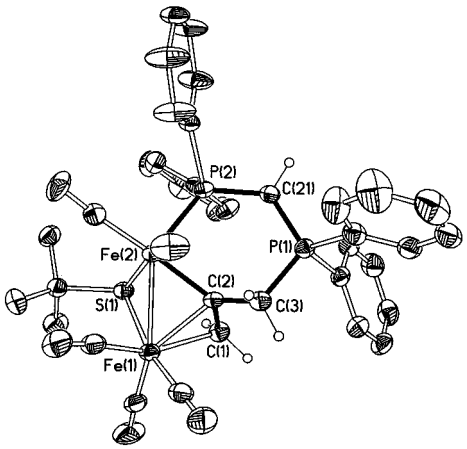

Figure 4. Molecular structure of $[Fe_2(CO)_5(\mu\text{-}S^tBu)\{\mu\text{-}\eta^1(P):\eta^1(C):\eta^2(C)\text{-}Ph_2PCHPPh_2CH_2C{=}CH_2\}]$ (**5b**), highlighting the six-membered ring formed by the "phosphine tethered" $\mu\text{-}\eta^1(P):\eta^1(C):\eta^2(C)$-coordinated alkenyl ligand. Phenyl and *tert*-butyl hydrogen atoms have been omitted.

Table 4. Selected Bond Distances (Å) and Angles (deg) for Compound 5b

Fe(1)−Fe(2)	2.5439(6)	Fe(1)−C(1)	2.157(3)
Fe(1)−C(2)	2.111(3)	Fe(2)−C(2)	1.987(3)
Fe(1)−S(1)	2.3061(8)	Fe(2)−S(1)	2.2589(8)
Fe(2)−P(2)	2.2082(9)	P(2)−C(21)	1.744(3)
C(21)−P(1)	1.682(3)	C(3)−P(1)	1.823(3)
C(1)−C(2)	1.400(4)	C(2)−C(3)	1.513(4)
Fe(2)−S(1)−Fe(1)	67.72(2)	P(2)−Fe(2)−S(1)	106.95(3)
C(21)−P(2)−Fe(2)	116.75(10)	P(1)−C(21)−P(2)	127.94(17)
C(21)−P(1)−C(3)	110.12(14)	C(2)−C(3)−P(1)	107.38(19)
C(3)−C(2)−Fe(2)	120.13(19)	C(2)−Fe(2)−P(2)	86.24(8)
C(1)−C(2)−C(3)	113.8(2)		

alkenyl ligand, σ-bonded to Fe(2) (Fe(2)−C(2) = 2.017(12) Å) and π-bonded to Fe(1) (Fe(1)−C(2) = 2.072(11) Å, Fe(1)−C(3) = 2.106(11) Å). Complex **5a**, a structural analogue of **4**, is derived from **2** *via* P−C_α bond formation, activation of a dppm methylene C−H bond coupled with hydrogen transfer to C_γ, and coordination of the remaining phosphorus to Fe(1) to generate a partially unsaturated five-membered ring. The phosphorus−carbon bonds of the bis(diphenylphosphino)methanide fragment in **5a** (P(1)−C(16) = 1.661(13) Å, P(2)−C(16) = 1.730(14) Å) are considerably shorter than the corresponding ones in **3** and similar to those in **4**, consistent with a degree of multiple bonding in the P−C−P fragment. A number of transition-metal bis(diphenylphosphino)methanide complexes have been crystallographically characterized, and in each case similar bond length reductions have been noted compared with their neutral dppm counterparts.[11,12] A single-crystal X-ray analysis identified **5b** as $[Fe_2(CO)_5(\mu\text{-}S^tBu)\{\mu\text{-}\eta^1(P):\eta^1(C):\eta^2(C)\text{-}Ph_2PCHPPh_2CH_2C{=}CH_2\}]$, an isomer of **5a** by virtue of competitive 1,3-hydrogen migration to C_α of the $\mu\text{-}\eta^1:\eta^2$-allenyl in **2**. In addition, **5a** and **5b** also exhibit coordination isomerism in that the σ-π-alkenyl ligand of **5b** is η^2-coordinated to the unsubstituted $Fe(CO)_3$ fragment (Fe(1)−C(2) = 2.111(3) Å, Fe(1)−C(1) = 2.157(3) Å), while in **5a** this ligand is η^2-coordinated to the phosphine-tethered iron (Scheme 1). Atoms P(1), C(3), C(2), Fe(2), P(2), and C(21) form a six-membered-ring system containing the bis(diphenylphosphino)-methanide (P(2)−C(21) = 1.744(3) Å, P(1)−C(21) = 1.682(3) Å) whose P−C bonds are comparable in length to those of **4** and **5a**. The most notable difference between **5a** and **5b** lies in the isomeric $\mu\text{-}\eta^1$: η^2-alkenyl ligands, whose coordination isomerism manifests itself in the formation of the five- and six-membered rings of **5a** and **5b**, respectively. At this time we tentatively suggest the selectivity for **5a** to be electronic in origin (η^2-coordination to a phosphine-substituted iron), together with a contribution from the inherent stability of five-membered rings. The remainder of the structure is as expected for a diiron sulfido-bridged σ-π-alkenyl complex. We suggest that **5a** and **5b** form *via* C−H activation and hydrogen migration in an η^2-allene intermediate similar to **3**, the final isomeric distribution depending upon the regiochemistry of hydrogen migration (Scheme 1).

The regioselective attack of neutral phosphorus-based nucleophiles at C_α of the $\mu\text{-}\eta^1:\eta^2$-allenyl ligand in $[Fe_2(CO)_6(\mu\text{-}PPh_2)\{\mu\text{-}\eta^1:\eta^2{}_{\alpha,\beta}\text{-}(H)C_\alpha{=}C_\beta{=}C_\gamma H_2\}]$ (**1**) contrasts sharply with previous reports of exclusive attack of carbon, phosphorus, and nitrogen nucleophiles at C_β of binuclear $\mu\text{-}\eta^1:\eta^2$- and mononuclear η^3-allenyl complexes.[7u,16] For instance, in all cases $[Ru_2(CO)_6(\mu\text{-}PPh_2)\{\mu\text{-}\eta^1:\eta^2{}_{\alpha,\beta}\text{-}(Ph)C_\alpha{=}C_\beta{=}C_\gamma H_2\}]$ reacts with monofunctional nucleophiles to form dimetallacyclopentanes and pentenes *via* attack at C_β.[7u] However, EHMO calculations on the model compound $[Ru_2(CO)_6(\mu\text{-}PH_2)\{\mu\text{-}\eta^1:\eta^2{}_{\alpha,\beta}\text{-}(H)C_\alpha{=}C_\beta{=}C_\gamma H_2\}]$ have shown that a significant component of the lowest unoccupied molecular orbital (LUMO) is centered on C_α and the lack of reactivity at this carbon was suggested to be steric in origin. The selectivity of $[Ru_2(CO)_6(\mu\text{-}PPh_2)\{\mu\text{-}\eta^1:\eta^2{}_{\alpha,\beta}\text{-}(Ph)C_\alpha{=}C_\beta{=}C_\gamma H_2\}]$ for nucleophilic attack at C_β was eventually rationalized by examining the characteristics of the LUMO and HOMO during rotation about C_β−C_γ, a dynamic process thought to be responsible for the exchange of the methylene protons. These studies showed that the orbital contribution to the LUMO from C_β maximizes at a rotation of the $C_\gamma H_2$ fragment of 88° with respect to the CH_2 plane in the ground state. Moreover, during this rotation a positive charge also develops on C_β, which suggests that overall the reactivity of $[Ru_2(CO)_6(\mu\text{-}PPh_2)\{\mu\text{-}\eta^1:\eta^2{}_{\alpha,\beta}\text{-}(Ph)C_\alpha{=}C_\beta{=}C_\gamma H_2\}]$ toward neutral nucleophiles is controlled by both orbital and charge factors. The highly regioselective attack of phosphorus-based nucleophiles at C_α of the $\mu\text{-}\eta^1:\eta^2{}_{\alpha,\beta}$-allenyl ligand in **1** prompted us to perform preliminary EHMO calculations[17] on the model compound $[Fe_2(CO)_6(\mu\text{-}PH_2)\{\mu\text{-}\eta^1:\eta^2{}_{\alpha,\beta}\text{-}(H)C_\alpha{=}C_\beta{=}C_\gamma H_2\}]$ using parameters derived from the X-ray structure of $[Fe_2(CO)_6(\mu\text{-}PPh_2)\{\mu\text{-}\eta^1:\eta^2{}_{\alpha,\beta}\text{-}(H)C_\alpha{=}C_\beta{=}C_\gamma H_2\}]$.[18] These calculations reveal that in the ground state, as for $[Ru_2(CO)_6(\mu\text{-}PPh_2)\{\mu\text{-}\eta^1:\eta^2{}_{\alpha,\beta}\text{-}(Ph)C_\alpha{=}C_\beta{=}C_\gamma H_2\}]$, the LUMO has a

(16) For comprehensive reviews on transition-metal allenyl chemistry see: (a) Doherty, S.; Corrigan, J. F.; Carty, A. J.; Sappa, E. *Adv. Organomet. Chem.* **1995**, *37*, 39. (b) Wojcicki, A. *New J. Chem.* **1994**, *18*, 61. For specific examples see: (c) Baize, M. W.; Blosser, P. W.; Plantevin, V.; Schimpff, D. G.; Gallucci, J. C.; Wojcicki, A. *Organometallics* **1996**, *15*, 164. (d) Baize, M. W.; Plantevin, V.; Gallucci, J. C.; Wojcicki, A. *Inorg. Chim. Acta* **1995**, *235*. 1. (e) Ogoshi, S.; Tsutsumi, K.; Kurosawa, H. *J. Organomet. Chem.* **1995**, *493*, C19. (f) Su, C.-C.; Chen, J.-T.; Lee, G.-H.; Wang, Y. *J. Am. Chem. Soc.* **1994**, *116*, 4999. (g) Huang, T.-M.; Chen, J.-T.; Lee, G.-H.; Wang, Y. *J. Am. Chem. Soc.* **1993**, *115*, 1170. (h) Blosser, P. W.; Schimpff, D. G.; Gallucci, J. C.; Wojcicki, A. *Organometallics* **1994**, *12*, 1993. (i) Huang, T.-M.; Hsu, R.-H.; Yang, C.-S.; Chen, J.-T.; Lee, G.-H.; Wang, Y. *Organometallics* **1994**, *13*, 3657. (j) Plantevin, V.; Blosser, P. W.; Gallucci, J. C.; Wojcicki, A. *Organometallics* **1994**, *13*, 3651.

(17) (a) Mealli, C.; Proserpio, D. M. *J. Chem. Educ.* **1990**, *67*, 399. (b) Hoffmann, R.; Lipscomb, W. N. *J. Chem. Phys.* **1962**, *36*, 2179, 3489. (c) Hoffmann, R. *J. Chem. Phys.* **1963**, *39*, 1397.

(18) Doherty, S.; Corrigan, J. F.; Waugh, M. Unpublished results.

large component centered on C_α, suggesting that the selectivity of **1** for nucleophilic attack at this carbon is under orbital control. Thus, in contrast to $[Ru_2(CO)_6(\mu\text{-}PPh_2)\{\mu\text{-}\eta^1\text{:}\eta^2_{\alpha,\beta}\text{-}(Ph)C_\alpha{=}C_\beta{=}C_\gamma H_2\}]$, in the absence of steric congestion, C_α in **1** and **2** is, at least for phosphorus-based nucleophiles, the preferred site of attack. Other significant contributions to the LUMO include Fe−CO nonbonding interactions and a small contribution to C_γ.

Conclusion

The diiron allenyl complex $[Fe_2(CO)_6(\mu\text{-}PPh_2)\{\mu\text{-}\eta^1\text{:}\eta^2_{\alpha,\beta}\text{-}(H)C_\alpha{=}C_\beta{=}C_\gamma H_2\}]$ (**1**) reacts with bis(diphenylphosphino)methane to afford, in the first instance, $[Fe_2(CO)_5(\mu\text{-}PPh_2)\{\eta^1(P)\text{:}\eta^2(C)\text{-}Ph_2PCH_2PPh_2(H)C{=}C{=}CH_2\}]$ (**3**), which, when left standing in toluene, slowly decarbonylates to give $[Fe_2(CO)_5(\mu\text{-}PPh_2)\{\mu\text{-}\eta^1(P)\text{:}\eta^1(C)\text{:}\eta^2(C)\text{-}Ph_2PCHPPh_2(H)C{=}CCH_3\}]$ (**4**). In contrast, dppm reacts with $[Fe_2(CO)_6(\mu\text{-}S^tBu)\{\mu\text{-}\eta^1\text{:}\eta^2_{\alpha,\beta}\text{-}(H)C_\alpha{=}C_\beta{=}C_\gamma H_2\}]$ (**2**) to afford the isomeric σ-π-alkenyl complexes $[Fe_2(CO)_5(\mu\text{-}S^tBu)\{\mu\text{-}\eta^1(P)\text{:}\eta^1(C)\text{:}\eta^2(C)\text{-}Ph_2PCHPPh_2(H)C{=}CCH_3\}]$ (**5a**) and $[Fe_2(CO)_5(\mu\text{-}S^tBu)\{\mu\text{-}\eta^1(P)\text{:}\eta^1(C)\text{:}\eta^2(C)\text{-}Ph_2PCHPPh_2CH_2C{=}CH_2\}]$ (**5b**). In each case the alkenyl ligand in **4**, **5a**, and **5b** presumably results from nucleophilic attack at C_α of the allenyl ligand and activation of a dppm methylene carbon−hydrogen bond in an intermediate η^2-dppm-functionalized allene complex, coupled with hydrogen migration to either C_γ (**4**, **5a**) or C_α (**5b**). These studies support our previous report of regiospecific nucleophilic attack of protic phosphines at C_α of the allenyl ligand in $[Fe_2(CO)_6(\mu\text{-}PPh_2)\{\mu\text{-}\eta^1\text{:}\eta^2_{\alpha,\beta}\text{-}(H)C_\alpha{=}C_\beta{=}C_\gamma H_2\}]$ (**1**), although, in contrast to phosphines with labile P−H bonds, dppm reacts *via* activation of its methylene C−H bond with hydrogen migration to the σ-η-hydrocarbon. These results further broaden the wealth of reactivity associated with transition-metal allenyl complexes. Additionally, we have identified new reaction pathways for dppm, a ligand that has until recently been assumed to adopt a role as an innocent spectator. We anticipate that new and exciting developments will continue to evolve from future endeavors in this area.

Experimental Section

General Procedures. Unless otherwise stated, all manipulations were carried out in an inert-atmosphere glovebox or by using standard Schlenk line techniques. Diethyl ether and hexane were distilled from Na/K alloy, tetrahydrofuran from potassium, and dichloromethane from CaH_2. $CDCl_3$ was predried with CaH_2 and vacuum-transferred and stored over 4 Å molecular sieves. Infrared spectra were recorded on a Mattson Genesis FTIR spectrometer operating WINFIRST software. Ultraviolet photolysis was carried out using a Hanovia medium-pressure lamp. Bis(diphenylphosphino)-methane, dodecacarbonyltriiron, and pentacarbonyliron were purchased from Strem Chemical Co. and used without further purification. The allenyl complexes $[Fe_2(CO)_6(\mu\text{-}PPh_2)\{\mu\text{-}\eta^1\text{:}\eta^2_{\alpha,\beta}\text{-}(H)C_\alpha{=}C_\beta{=}C_\gamma H_2\}]$[8] and $[Fe_2(CO)_6(\mu\text{-}S^tBu)\{\mu\text{-}\eta^1\text{:}\eta^2_{\alpha,\beta}\text{-}(H)C_\alpha{=}C_\beta{=}C_\gamma H_2\}]$[19] were prepared as previously described.

Preparation of $[Fe_2(CO)_6(\mu\text{-}PPh_2)\{\eta^1(P)\text{:}\eta^2(C)\text{-}Ph_2PCH_2PPh_2(H)C{=}C{=}CH_2\}]$ (3). A slight excess of dppm (0.115 g, 0.35 mmol) was added to a rapidly stirred solution of **1** (0.150 g, 0.3 mmol) in toluene/diethyl ether (30/30 mL). After all the dppm had dissolved, stirring was stopped and the reaction mixture left to stand overnight, during which time the solution changed from yellow to orange-red. After 20 h the large quantity of crystalline material deposited on the bottom of the flask was isolated and dried in *vacuo* to afford **3** in 60% yield (0.160 g). IR (ν(CO), cm^{-1}, CH_2Cl_2): 2022 m, 1982 m, 1921 s. $^{31}P\{^1H\}$ NMR (202 MHz, CD_2Cl_2, δ): 75.6 (ABX, $^2J_{PP}$ = 96.9 Hz, $^2J_{PP}$ = 54.0 Hz, Fe−PPh_2), 73.7 (ABX, $^2J_{PP}$ = 96.9 Hz, $^2J_{PP}$ = 29.6 Hz, μ-PPh_2), 37.8 (ABX, $^2J_{PP}$ = 54.0 Hz, $^2J_{PP}$ = 29.6 Hz, C−PPh_2−C). ^1H NMR (500.1 MHz, CD_2Cl_2, δ): 8.0−7.0 (m, C_6H_5, 30 H), 6.00 (br, s, 1H, C=C$H_a$$H_b$), 5.41 (br, s, 1H, C=C$H_a$$H_b$), 3.31 (m, 1H, P−C$H_2$−P), 2.01 (m, 2H, P−C$H_2$−P and *H*C=C). $^{13}C\{^1H\}$ NMR (125.1 MHz, $CDCl_3$, δ): 216.8 (d, $^2J_{PC}$ = 14.3 Hz, CO), 215.2 (d, $^2J_{PC}$ = 12.0 Hz, CO), 147.5 (dd, $^2J_{PC}$ = 62.9 Hz, $^2J_{PC}$ = 15.3 Hz, *C*=CH_2), 136−127 (m, C_6H_5), 121.0 (s, CC=*C*H_2), 25.2 (dd, $^1J_{PC}$ = 69.9 Hz, $^1J_{PC}$ = 5.7 Hz, P*C*H_2P), 18.2 (d, $^1J_{PC}$ = 65.3 Hz, *C*HC=CH_2). Anal. Calcd for $C_{46}H_{35}Fe_2O_6P_3$: C, 62.16; H, 3.97. Found: C, 62.65; H, 4.19.

UV Photolysis of $[Fe_2(CO)_6(\mu\text{-}PPh_2)\{\eta^1(P)\text{:}\eta^2(C)\text{-}Ph_2PCH_2PPh_2(H)C{=}C{=}CH_2\}]$ (4). A solution of **3** (0.120 g, 0.14 mmol) in toluene (150 mL) was irradiated for 30 min, during which time the color changed from pale yellow to deep orange. The solvent was removed under reduced pressure to afford an orange solid which when crystallized from dichloromethane/*n*-hexane gave **4** in 90% yield (0.105 g). IR (ν(CO), cm^{-1}, C_6H_{14}): 2046 w, 2030 s, 1974 s, 1953 m, 1917 w. $^{31}P\{^1H\}$ NMR (202 MHz, $CDCl_3$, δ): 185.5 (dd, $^2J_{PP}$ = 63.0 Hz, $^3J_{PP}$ = 39.0 Hz, μ-PPh_2), 66.0 (dd, $^2J_{PP}$ = 122.0 Hz, $^2J_{PP}$ = 63.0 Hz, Fe−PPh_2), 34.2 (dd, $^2J_{PP}$ = 122.0 Hz, $^3J_{PP}$ = 39.0 Hz, C−PPh_2−C). ^1H NMR (500.1 MHz, $CDCl_3$, δ): 8.0−7.1 (m, 30H, C_6H_5), 2.47 (s, 3H, C=CCH_3), 1.92 (q, $^2J_{PH}$ = $^3J_{PH}$ = 11.0 Hz, 1H, *H*C=CCH$_3$), 1.65 (dd, $^2J_{PH}$ = 13.7 Hz, $^2J_{PH}$ = 8.5 Hz, 1H, P−C*H*−P) $^{13}C\{^1H\}$ NMR (125.1 MHz, $CDCl_3$, δ): 220.4 (d, $^2J_{PC}$ = 24.0 Hz, CO), 217.0 (d, $^2J_{PC}$ = 22.0 Hz, CO), 211.3 (s, CO), 197.5 (d, $^2J_{PC}$ = 11.1 Hz, C=*C*Me), 145−128 (m, C_6H_5), 56.5 (dd, $^1J_{PC}$ = 75.3 Hz, $^2J_{PC}$ = 9.8 Hz, H*C*=CMe), 40.4 (br m, HC=C*C*H$_3$), 3.2 (dd, $^1J_{PC}$ = 133.4 Hz, $^1J_{PC}$ = 63.7 Hz, $Ph_2PCHPPh_2$). Anal. Calcd for $C_{45}H_{35}Fe_2O_5P_3$: C, 62.79; H, 4.10. Found C, 62.80; H, 4.23.

Preparation of $[Fe_2(CO)_5(\mu\text{-}S^tBu)\{\mu\text{-}\eta^1(P)\text{:}\eta^1(C)\text{:}\eta^2(C)\text{-}Ph_2PC(H)PPh_2(H)C{=}CCH_3\}]$ (5a) and $[Fe_2(CO)_5(\mu\text{-}S^tBu)\{\mu\text{-}\eta^1(P)\text{:}\eta^1(C)\text{:}\eta^2(C)\text{-}Ph_2PCHPPh_2CH_2C{=}CH_2\}]$ (5b). A solution of dppm (0.245 g, 0.64 mmol) in diethyl ether (20 mL) was added *via* cannula to a rapidly stirred solution of $[Fe_2(CO)_6(\mu\text{-}S^tBu)\{\mu\text{-}\eta^1\text{:}\eta^2_{\alpha,\beta}\text{-}(H)C_\alpha{=}C_\beta{=}C_\gamma H_2\}]$ (0.260 g, 0.64 mmol) in diethyl ether (30 mL) with monitoring of the reaction by TLC and IR spectroscopy. A deep cherry red color appeared immediately, and the reaction was complete within minutes. After the solvent was removed, the resultant oily residue was extracted with hexane (3 × 30 mL) to give a clear red solution which upon concentration (~10 mL) and cooling at −20 °C afforded a mixture of deep red (**5a**) and orange (**5b**) crystals in a combined yield of 69% (0.336 g). Isomers **5a** and **5b** were separated mechanically under an optical microscope.

Compound **5a**: IR (ν(CO), cm^{-1}, C_6H_{14}) 2038 s, 1984 s, 1965 s, 1916 m; $^{31}P\{^1H\}$ NMR (202 MHz, $CDCl_3$, δ) 61.8 (d, $^2J_{PP}$ = 112.0 Hz, Fe−PPh_2), 25.9 (d, $^2J_{PP}$ = 112.0 Hz, C−PPh_2−C); ^1H NMR (500.1 MHz, C_6D_6, δ) 8.35 (dd, $^3J_{HH}$ = 7.1 Hz, $^3J_{PH}$ = 8.0 Hz, 2H, *ortho*), 8.31 (dd, $^3J_{HH}$ = 8.3 Hz, $^3J_{PH}$ = 9.4 Hz, 2H, *ortho*), 8.11 (dd, $^2J_{HH}$ = 8.4 Hz, $^3J_{PH}$ = 9.1 Hz, 2H, *ortho*), 7.80 (m, 2H, *ortho*), 7.5−7.1 (m, 12H, C_6H_5), 2.85 (d, $^4J_{PH}$ = 4.2 Hz, 3H, C*H*$_3$), 2.83 (dd, $^2J_{PH}$ = 16.0 Hz, $^3J_{PH}$ = 11.2 Hz, 1H, C*H*=CCH$_3$), 1.94 (dd, $^2J_{PH}$ = 13.0 Hz, $^2J_{PH}$ = 8.9 Hz, 1H, P−C*H*−P), 1.61 (s, 9H, C(C*H*$_3$)$_3$); $^{13}C\{^1H\}$ NMR (125.1 MHz, $CDCl_3$, δ) 220.0 (d, $^2J_{PC}$ = 24.0 Hz, CO), 217.0 (d, $^2J_{PC}$ = 22.0 Hz, CO), 211.0 (s, CO), 198.3 (d, $^2J_{PC}$ = 10.0 Hz, C=*C*Me), 145−128 (m, C_6H_5), 57.9 (d, $^1J_{PC}$ = 75.0 Hz, H*C*=CMe), 48.7 (s, S*C*(CH$_3$)$_3$), 41.3 (dd, $^2J_{PC}$ = 11.3 Hz, $^2J_{PC}$ = 3.8 Hz, HCC*C*H$_3$), 33.2 (s, SC(*C*H$_3$)$_3$), 8.6 (dd, $^1J_{PC}$ = 135.7 Hz, $^1J_{PC}$ = 66.6 Hz, $Ph_2PCHPPh_2$). Anal. Calcd for $C_{37}H_{34}Fe_2O_5P_2S$: C, 58.20; H, 4.48. Found C, 58.57; H, 4.13.

(19) Seyferth, D.; Womack, C. M.; Dewan, J. C. *Organometallics* **1989**, *8*, 430.

Table 5. Summary of Crystal Data and Structure Determination for Compounds 3, 4, 5a, and 5b

	3·$^1/_2$ toluene	**4**·CH_2Cl_2·$^1/_2$ hexane	**5a**	**5b**
mol formula	$C_{46}H_{33}Fe_2O_6P_3$·$0.5C_7H_8$	$C_{45}H_{35}Fe_2O_5P_3$·CH_2Cl_2·$0.5C_6H_{14}$	$C_{37}H_{34}Fe_2O_5P_2S$	$C_{37}H_{34}Fe_2O_5P_2S$
fw	932.4	988.4	764.3	764.3
temp, K	160	160	160	160
cryst syst	triclinic	triclinic	monoclinic	triclinic
space group	$P\bar{1}$	$P\bar{1}$	$P2_1$	$P\bar{1}$
a, Å	11.3498(12)	11.8979(11)	17.5589(14)	10.2099(13)
b, Å	12.0803(13)	12.2293(11)	11.2530(9)	10.7921(14)
c, Å	17.730(2)	15.9827(15)	18.5709(15)	18.496(2)
α, deg	87.624(3)	99.440(2)		78.025(3)
β, deg	78.363(3)	103.827(2)	106.046(2)	85.654(3)
γ, deg	65.475(3)	96.506(2)		62.876(4)
V, Å^3	2163.8(4)	2199.1(4)	3526.5(5)	1774.0(4)
Z	2	2	4	2
D_{calcd}, g cm^{-3}	1.431	1.489	1.440	1.431
μ(Mo Kα), cm^{-1}	8.32	9.38	10.14	10.08
cryst size, mm	0.39 × 0.06 × 0.06	0.22 × 0.17 × 0.06	0.72 × 0.46 × 0.45	0.34 × 0.22 × 0.06
transmissn coeff range	0.790−0.952	0.671−0.928	0.726−0.887	0.796−0.959
scan range (2θ), deg	4.3−50.0	2.7−50.0	2.3−45.0	4.3−57.0
no. of rflns measd	11 402	12 612	15 053	10 987
no. of unique rflns	7517	7556	9114	7687
R_{int}	0.0436	0.0621	0.0391	0.0368
weighting parameters[a] a, b	0.0370, 12.4648	0.0638, 0	0.0272, 55.4463	0.0387, 0.8536
extinction coeff x[b]	0.0009(4)	0.0008(5)	0.0006(2)	0.0008(4)
no. of variables	575	587	858	434
no. of restraints	65	61	75	0
R_w (all data)[c]	0.1786	0.1566	0.1899	0.0957
R ("observed" data)[d]	0.0746 (5667)	0.0687 (4407)	0.0749 (8996)	0.0407 (5306)
GOF[e]	1.107	0.982	1.155	1.011
max, min electron density, e Å^{-3}	+1.50, −0.96	+0.70, −0.57	+1.82, −0.68	+0.39, −0.34

[a] $w^{-1} = \sigma^2(F_o^2) + (aP)^2 + bP$, where $P = (F_o^2 + 2F_c^2)/3$. [b] $F_c' = F_c(1 + xF_c^2\lambda^3/\sin 2\theta)^{-1/4}$. [c] $R_w = \{\sum[w(F_o^2 - F_c^2)^2]/\sum[w(F_o^2)^2]\}^{1/2}$ for all data. [d] $R = \sum||F_o| - |F_c||/\sum|F_o|$ for reflections having $F_o^2 > 2\sigma(F_o^2)$. [e] GOF = $[\sum w(F_o^2 - F_c^2)^2/((\text{no. of unique rflns}) - (\text{no. of variables}))]^{1/2}$.

Compound **5b**: IR (ν(CO), cm^{-1}, C_6H_{14}): 2053 sh, 2038 m, 1976 s, 1920 w; $^{31}P\{^1H\}$ NMR (202 MHz, $CDCl_3$, δ) 60.6 (d, $^2J_{PP}$ = 72.0 Hz, Fe−PPh_2), 30.4 (d, $^2J_{PP}$ = 72.0 Hz, C−PPh_2−C); ^1H NMR (500.1 MHz, C_6D_6, δ) 7.8−7.1 (m, C_6H_5, 20 H), 4.20 (t, $^2J_{HH}$ = 12.4 Hz, $^2J_{PH}$ = 4.2 Hz, 1H, CH_aH_b), 3.31 (t, $^2J_{HH}$ = 12.7 Hz, $^2J_{PH}$ = 4.2 Hz, 1H, CH_aH_b), 3.15 (d, br, $^2J_{HH}$ = 2.0 Hz, 1H, CH_cH_d), 2.65 (d, br, $^2J_{HH}$ = 2.0 Hz, 1H, CH_cH_d), 1.80 (t, $^2J_{PC}$ = 7.8 Hz, 1H, P−C*H*−P), 0.98 (s, 9H, C(CH_3)$_3$). Anal. Calcd for $C_{37}H_{34}Fe_2O_5P_2S$: C, 58.20; H, 4.48. Found: C, 58.61; H, 4.27.

Crystal Structure Determination of 3, 4, 5a, and 5b. Single crystals of each compound were obtained by crystallization: from toluene/diethyl ether for **3** and CH_2Cl_2/*n*-hexane for **4**, **5a**, and **5b**. Crystals were examined on a Siemens SMART CCD area-detector diffractometer with graphite-monochromated Mo Kα radiation (λ = 0.710 73 Å). Cell parameters were refined from the observed setting angles of all strong reflections in each complete data set. Intensities were integrated from series of ω-rotation exposures with different ϕ-angles chosen to generate more than a hemisphere of data, each exposure covering 0.3° in ω. Analysis of repeated and symmetry-equivalent data indicated no significant intensity decay and formed the basis of empirical absorption corrections.

The structures were solved by direct methods and refined by full-matrix least squares on F^2 values for all unique data (see Table 5 for details). All non-hydrogen atoms except for hexane solvent were assigned anisotropic displacement parameters. Hydrogen atoms were constrained to ideal positions with a riding model and with U_{iso}(H) set at 1.2 (1.5 for methyl groups) times U_{eq} for the parent atom, except for allene and alkene CH and CH_2, for which positions were refined freely. For **3**, a disordered toluene was located and refined with restraints on geometry and displacement parameters; hydrogen atoms were not included. For **4**, disordered CH_2Cl_2 and *n*-hexane molecules were located and refined, also with appropriate restraints and with H atoms for CH_2Cl_2 only. The structure of **5a** was found to be partially twinned racemically. Programs used were Siemens SMART (control) and SAINT (integration) software,[20] SHELXTL,[21] and local programs, on Silicon Graphics Indy workstations and personal computer systems.

Acknowledgment. We thank the University of Newcastle, the Nuffield Foundation, and the Royal Society for financial support (S.D.) and the EPSRC for funding for a diffractometer (W.C.). We thank Dr. John F. Corrigan for his assistance with the molecular orbital calculations and helpful discussions.

Supporting Information Available: For **3**, **4**, **5a**, and **5b,** details of the structure determination (Tables S1, S6, S11, and S16), non-hydrogen atom positional parameters (Tables S2, S7, S12, and S17), bond distances and angles (Tables S3, S8, S13, and S18), anisotropic displacement parameters (Tables S4, S9, S14, and S19), and hydrogen atom parameters (Tables S5, S10, S15, and S20) (36 pages). Ordering information is given on any current masthead page. Observed and calculated structure factors are available from the authors upon request.

OM960502E

(20) SMART and SAINT software for CCD diffractometers, from Siemens Analytical X-ray Instruments Inc., Madison, WI, 1995.
(21) Sheldrick, G. M. *SHELXTL Manual, Version 5*, Siemens Analytical X-ray Instruments: Madison, WI, 1994.